Anal. Chem. **2010,** *82,* 8235–8243

Development of a Troponin I Biosensor Using a Peptide Obtained through Phage Display

Jun Wu,[†,‡] Donald M. Cropek,[‡] Alan C. West,[†] and Scott Banta*[,†]

Department of Chemical Engineering, Columbia University, New York, New York, and U.S. Army Engineer Research and Development Center, Construction Engineering Research Laboratory (CERL), Champaign, Illinois

A small synthetic peptide with nanomolar affinity for cardiac troponin I (TnI), previously identified from a polyvalent phage displayed library, has been immobilized on a gold surface for TnI detection. The binding affinity of gold-immobilized peptides for TnI was studied and compared with that of phage-immobilized peptides. Quartz crystal microbalance (QCM), cyclic voltammetry, and electrochemical impedance spectroscopy (EIS) were used to monitor both the immobilization and target binding processes. All three techniques show that the binding is specific for TnI as compared to a streptavidin (SA) control. The response curves obtained at TnI concentrations ranging from 0 to 10 μg/mL, using both QCM and EIS, were also compared. For the EIS measurements, the sensitivity was 0.30 ± 0.030 normalized impedance/(μg/mL) and the limit of detection (LOD) was 0.34 μg/mL. Using the QCM, a sensitivity of 18 ± 1 Hz/(μg/mL) was obtained, corresponding to an LOD of 0.11 μg/mL. Although the QCM demonstrated a lower LOD as compared to EIS, the latter technique exhibited a larger linear dynamic range than QCM. In a relevant tissue culture milieu, Minimum Essential Media (MEM), the sensitivity of the EIS measurement was greater than that obtained in a phosphate buffer system (PBS). The kinetics of target binding using QCM were analyzed by two independent methods, and the dissociation constants (K_D = 66 ± 4 nM and 17 ± 8 nM) were an order of magnitude higher than that calculated for the polyvalent phage particles (K_D = 2.5 ± 0.1 nM). Even though the affinity of the immobilized peptides for TnI was somewhat reduced, overall, these results demonstrate that peptides obtained from the biopanning of phage display libraries can be readily used as sensing probes in biosensor development.

Cardiac troponin I (TnI), with a molecular weight of 24 kDa,[1,2] is part of the troponin complex that is present in cardiac muscle tissues. For more than 15 years, TnI has been known as a reliable biomarker of cardiac muscle tissue injury and used in the early diagnosis of acute myocardial infarction (AMI).[3−8] Compared to other biomarkers, such as CK-MB, FABP3, myoglobin, and LDH isoenzymes, TnI has higher specificity and selectivity for AMI.[9−14] Following myocardial damage in AMI, the troponin complex releases TnI into the bloodstream. The TnI concentration in blood increases from ∼10 ng/mL in healthy people to a peak value as high as ∼100 ng/mL after 12−24 h. After 6−8 days, the TnI levels return to normal, and thus, this biomarker provides a long window for detection.[5,9,11,12,15]

Conventional enzyme-linked immunosorbent assays (ELISA) are most frequently used for quantitative detection of TnI, and the commercially available sensors have limits of detection (LOD) ranging from 0.001 to 0.1 ng/mL.[9,16−18] Other TnI sensors have been reported using fluorescence resonance energy transfer (FRET; LOD, 1−800 ng/mL)[19,20] and electrochemical techniques such as anodic stripping voltammetry and cyclic voltammetry (LOD, 0.1−0.5 ng/mL).[21,22] These techniques rely on antibodies for biomolecular recognition and require multistep processing and labeling of the samples. We have recently identified a 12 amino acid peptide that specifically binds to TnI with nanomolar affinity

* Corresponding author. E-mail: sbanta@columbia.edu. Phone: (212) 854-7531. Fax: (212) 854-3054.

† Columbia University.

‡ CERL.

(1) Greaser, M. L.; Gergely, J. *J. Biol. Chem.* **1973**, *248*, 2125–2133.
(2) Labugger, R.; Organ, L.; Collier, C.; Atar, D.; Van Eyk, J. E. *Circulation* **2000**, *102*, 1221–1226.
(3) Adams, J. E.; Bodor, G. S.; Davilaroman, V. G.; Delmez, J. A.; Apple, F. S.; Ladenson, J. H.; Jaffe, A. S. *Circulation* **1993**, *88*, 101–106.
(4) Apple, F. S. *Cardiovasc. Toxicol.* **2001**, *1*, 93–98.
(5) Babuin, L.; Jaffe, A. S. *CMAJ* **2005**, *173*, 1191–1202.
(6) Eriksson, S.; Wittfooth, S.; Pettersson, K. *Crit. Rev. Clin. Lab. Sci.* **2006**, *43*, 427–495.
(7) Howie-Esquivel, J.; White, M. *J. Cardiovasc. Nurs.* **2008**, *23*, 124–131.
(8) Jaffe, A. S.; Babuin, L.; Apple, F. S. *J. Am. Coll. Cardiol.* **2006**, *48*, 1–11.
(9) McDonnell, B.; Hearty, S.; Leonard, P.; O'Kennedy, R. *Clin. Biochem.* **2009**, *42*, 549–561.
(10) O'Brien, P. J. *Toxicology* **2008**, *245*, 206–218.
(11) Casals, G.; Filella, X.; Bedini, J. L. *Clin. Biochem.* **2007**, *40*, 1406–1413.
(12) Melanson, S. E. F.; Conrad, M. J.; Mosammaparast, N.; Jarolim, P. *Clin. Chim. Acta* **2008**, *395*, 57–61.
(13) Panteghini, M. *Clin. Chem.* **2005**, *51*, 1594–1597.
(14) Wallace, K. B.; Hausner, E.; Herman, E.; Holt, G. D.; MacGregor, J. T.; Metz, A. L.; Murphy, E.; Rosenblum, I. Y.; Sistare, F. D.; York, M. J. *Toxicol. Pathol.* **2004**, *32*, 106–121.
(15) Jaffe, A. S.; Landt, Y.; Parvin, C. A.; Abendschein, D. R.; Geltman, E. M.; Ladenson, J. H. *Clin. Chem.* **1996**, *42*, 1770–1776.
(16) Collinson, P. O.; Boa, F. G.; Gaze, D. C. *Ann. Clin. Biochem.* **2001**, *38*, 423–449.
(17) Sodi, R. *Adv. Clin. Chem.* **2006**, *41*, 49–122.
(18) Mohammed, A. A.; Januzzi, J. L. *Cardiol. Rev. , 18*, 12–19.
(19) Heyduk, E.; Dummit, B.; Chang, Y. H.; Heyduk, T. *Anal. Chem.* **2008**, *80*, 5152–5159.
(20) Stringer, R. C.; Hoehn, D.; Grant, S. A. *IEEE Sens. J.* **2008**, *8*, 295–300.
(21) Guo, H. S.; He, N. Y.; Ge, S. X.; Yang, D.; Zhang, J. N. *Talanta* **2005**, *68*, 61–66.
(22) Ko, S.; Kim, B.; Jo, S.-S.; Oh, S. Y.; Park, J.-K. *Biosens. Bioelectron.* **2007**, *23*, 51–59.

10.1021/ac101657h
Published on Web 09/10/2010

using phage display technology.[23] Compared to more complex affinity scaffolds, short linear peptides have several advantages for biosensor development: (1) peptides can be synthesized easily and inexpensively; (2) peptides are more stable and resistant to harsh environments; and (3) peptides are more amenable than antibodies to engineering at the molecular level.[24−27] There have been some reports where the entire phage particles (with multiple copies of the peptides) are employed as the sensing probes on biosensors.[28−32] Although phage display has been widely applied to identify peptides or proteins with specific binding capabilities, the application of the free peptides in the development of biosensors is rarely reported.

The application of the chemically synthesized peptide rather than the polyvalent phage particle as the sensing moiety to detect target proteins is a valuable and versatile approach, but further studies on the transition from phage to peptide chip immobilization are required. For example, studies have been conducted with immobilized peptides identified by phage display to create sensors for camptothecin (CPT) and trinitrotoluene (TNT).[33−36] A multistep modification of the surface was needed for the peptide immobilization process. In this work, we have begun to determine a general and practical approach to use newly evolved peptides for biosensor application. A quartz crystal microbalance (QCM) and electrochemical techniques were used to monitor both the sensor surface preparation and subsequent binding properties of immobilized peptides for the target TnI.

QCM has been widely used in biosensors since it is regarded as a label-free technique.[34,37−42] It can detect the mass change, Δm, that is physically coupled or bound to the crystal surface by measuring the resonant frequency change, Δf, of the vibrating crystal. Many QCM instruments can also measure the dissipation energy, D, or crystal resistance, ΔR, providing supporting information related to the structure of the surface film. Another advantage of QCM is that it is a real-time and in situ technique, so that its output provides an indication of whether binding reaches a steady state at a specific time. The disadvantage of QCM is its sensitivity to extraneous environmental conditions, such as temperature and vibration, during the measurement.

Electrochemical techniques can also be used for the creation of label-free biosensors.[43−51] They are low-cost, fast responding, and require minimal maintenance. Electrodes can be easily integrated into microfabricated chips and used as portable test tools for field measurements.[48,52] Cyclic voltammetry (CV) and electrochemical impedance spectroscopy (EIS) are frequently used techniques. Depending on the electrolytes, two methods of performing EIS are often used.[53,54] In the first approach, a nonfaradaic or capacitive impedance is measured.[55−57] In the other approach, a faradaic impedance, using a redox couple such as the ferri/ferrocyanide couple, is measured. The nonfaradaic impedance measurement avoids the complexity resulting from the introduction of the redox couple but usually shows lower sensitivity than a faradaic impedance measurement.[45,46,53] For these measurements, increases in both the faradaic and nonfaradaic impedance are related to molecules (including TnI bound by peptide) that are adsorbed on the gold electrode. Both the density of attached molecules and their orientation impact the impedance by hindering current flow across the electrode/electrolyte interface.

The biosensors envisioned in the present study are intended for downstream detection of TnI produced from cardiac cell culture grown in microfluidic devices. The determination of the LOD of these biosensors is an important factor for consideration in the system design.[54] In vitro studies can be used to provide an estimate of the amount of TnI that will be produced by the cultured cells. For example, isolated rat cardiac cells in vitro have been shown to release ~80% of their initial TnI content into their culture media when the cells were exposed to toxic substances.[58,59] The

(23) Park, J. P.; Cropek, D. M.; Banta, S. *Biotechnol. Bioeng.* **2010**, *105*, 678–686.
(24) Dover, J. E.; Hwang, G. M.; Mullen, E. H.; Prorok, B. C.; Suh, S. J. *J. Microbiol. Methods* **2009**, *78*, 10–19.
(25) Iqbal, S. S.; Mayo, M. W.; Bruno, J. G.; Bronk, B. V.; Batt, C. A.; Chambers, J. P. *Biosens. Bioelectron.* **2000**, *15*, 549–578.
(26) Luong, J. H. T.; Male, K. B.; Glennon, J. D. *Biotechnol. Adv.* **2008**, *26*, 492–500.
(27) Luppa, P. B.; Sokoll, L. J.; Chan, D. W. *Clin. Chim. Acta* **2001**, *314*, 1–26.
(28) Archer, M. J.; Liu, J. L. *Sensors* **2009**, *9*, 6298–6311.
(29) Jia, Y. F.; Qin, M.; Zhang, H. K.; Niu, W. C.; Li, X.; Wang, L. K.; Bai, Y. P.; Cao, Y. J.; Feng, X. Z. *Biosens. Bioelectron.* **2007**, *22*, 3261–3266.
(30) Lakshmanan, R. S.; Guntupalli, R.; Hu, J.; Petrenko, V. A.; Barbaree, J. M.; Chin, B. A. *Sens. Actuators, B: Chem.* **2007**, *126*, 544–550.
(31) Liu, F. F.; Luo, Z. F.; Ding, X.; Zhu, S. G.; Yu, X. L. *Sens. Actuators, B: Chem.* **2009**, *136*, 133–137.
(32) Nanduri, V.; Sorokulova, I. B.; Samoylov, A. M.; Simonian, A. L.; Petrenko, V. A.; Vodyanoy, V. *Biosens. Bioelectron.* **2007**, *22*, 986–992.
(33) Samoylov, A. M.; Samoylova, T. I.; Hartell, M. G.; Pathirana, S. T.; Smith, B. F.; Vodyanoy, V. *Biomol. Eng.* **2002**, *18*, 269–272.
(34) Samoylov, A. M.; Samoylova, T. I.; Pathirana, S. T.; Globa, L. P.; Vodyanoy, V. J. *J. Mol. Recognit.* **2002**, *15*, 197–203.
(35) Cerruti, M.; Jaworski, J.; Raorane, D.; Zueger, C.; Varadarajan, J.; Carraro, C.; Lee, S. W.; Maboudian, R.; Majumdar, A. *Anal. Chem.* **2009**, *81*, 4192–4199.
(36) Takakusagi, Y.; Kobayashi, S.; Sugawara, F. *Bioorg. Med. Chem. Lett.* **2005**, *15*, 4850–4853.
(37) Cooper, M. A.; Singleton, V. T. *J. Mol. Recognit.* **2007**, *20*, 154–184.
(38) Marx, K. A. *Springer Ser. Chem. Sens. Biosens.* **2007**, *5*, 371–424.
(39) Laricchia-Robbio, L.; Revoltella, R. P. *Biosens. Bioelectron.* **2004**, *19*, 1753–1758.
(40) Melles, E.; Anderson, H.; Wallinder, D.; Shafqat, J.; Bergman, T.; Aastrup, T.; Jornvall, H. *Anal. Biochem.* **2005**, *341*, 89–93.
(41) Shen, Z. H.; Mernaugh, R. L.; Yan, N. P.; Yu, L.; Zhang, Y.; Zeng, X. Q. *Anal. Chem.* **2005**, *77*, 6834–6842.
(42) Shen, Z.; Stryker, G. A.; Mernaugh, R. L.; Yu, L.; Yan, H. P.; Zeng, X. Q. *Anal. Chem.* **2005**, *77*, 797–805.
(43) Chen, X. J. J.; West, A. C.; Cropek, D. M.; Banta, S. *Anal. Chem.* **2008**, *80*, 9622–9629.
(44) Lisdat, F.; Schafer, D. *Anal. Bioanal. Chem.* **2008**, *391*, 1555–1567.
(45) Mantzila, A. G.; Strongylis, C.; Tsikaris, V.; Prodromidis, M. I. *Biosens. Bioelectron.* **2007**, *23*, 362–369.
(46) Rickert, J.; Gopel, W.; Beck, W.; Jung, G.; Heiduschka, P. *Biosens. Bioelectron.* **1996**, *11*, 757–768.
(47) Bart, M.; Stigter, E. C. A.; Stapert, H. R.; de Jong, G. J.; van Bennekom, W. P. *Biosens. Bioelectron.* **2005**, *21*, 49–59.
(48) Curtis, T. M.; Widder, M. W.; Brennan, L. M.; Schwager, S. J.; van der Schalie, W. H.; Fey, J.; Salazar, N. *Lab Chip* **2009**, *9*, 2176–2183.
(49) Du, P.; Li, H. X.; Mei, Z. H.; Liu, S. F. *Bioelectrochemistry* **2009**, *75*, 37–43.
(50) Wegener, J.; Zink, S.; Rosen, P.; Galla, H. J. *Pfluegers Arch.-Eur. J. Physiol.* **1999**, *437*, 925–934.
(51) Luong, J. H. T. *Anal. Lett.* **2003**, *36*, 3147–3164.
(52) Ceriotti, L.; Ponti, J.; Colpo, P.; Sabbioni, E.; Rossi, F. *Biosens. Bioelectron.* **2007**, *22*, 3057–3063.
(53) Panke, O.; Balkenhohl, T.; Kafka, J.; Schafer, D.; Lisdat, F. *Adv. Biochem. Eng. Biotechnol.* **2008**, *109*, 195–237.
(54) Daniels, J. S.; Pourmand, N. *Electroanalysis* **2007**, *19*, 1239–1257.
(55) de Vasconcelos, E. A.; Peres, N. G.; Pereira, C. O.; da Silva, V. L.; da Silva, E. F., Jr.; Dutra, R. F. *Biosens. Bioelectron.* **2009**, 25.
(56) Berggren, C.; Bjarnason, B.; Johansson, G. *Electroanalysis* **2001**, *13*, 173–180.
(57) Saby, C.; Jaffrezicrenault, N.; Martelet, C.; Colin, B.; Charles, M. H.; Delair, T.; Mandrand, B. *Sens. Actuators, B:Chem.* **1993**, *16*, 458–462.
(58) Adamcova, M.; Simunek, T.; Kaiserova, H.; Popelova, O.; Sterba, M.; Potacova, A.; Vavrova, J.; Malakova, J.; Gersl, V. *Toxicology* **2007**, *237*, 218–228.

packing of cells within the device, the geometric and microfluidic designs, and the mode of operation of the chip will ultimately determine the analyte concentration range that will need to be detected using these sensors.

In this report, we aim to provide a more general approach to the utilization of peptides identified by biopanning of phage displayed libraries for biosensor applications. The selected peptides were immobilized on gold surface via cysteine amino acid added to the C-terminus of the peptide. The response curves obtained using QCM and EIS were compared. The QCM measurements resulted in a lower LOD, but EIS shows a larger linear response range. The kinetics of the binding of the TnI target using QCM were used to obtained binding constants, and these were compared to binding constants using peptides left on the phage particles. The results demonstrate that peptides obtained from phage display experiments can be readily incorporated onto gold surfaces for use in biosensor development.

EXPERIMENTAL DETAILS

Reagents and Solutions. All reagents in this work were analytical grade unless otherwise stated. Troponin I (TnI, human heart) was obtained from Lee Biosolutions, Inc. (St. Louis, Missouri). Streptavidin (SA) from *Streptomyces avidinii* and L-cysteine hydrochloride (98%) were obtained from Sigma-Aldrich (St. Louis, MO). Peptides (90% purity) for binding of TnI (TnPep, sequence: FYSHSFHENWPS-Cys) and for binding SA (SAPep, sequence: WSHPQFEKGSGS-Cys) were synthesized by Genscript (Piscataway, NJ). Buffer solutions (pH = 7) containing 0.1 M phosphate, 0.25 M NaCl, and 1 mM EDTA were used to make all protein (1−10 μg/mL) and peptide (0.1 mM) buffer solutions unless otherwise stated. Minimum Essential Medium (MEM) was obtained from Sigma-Aldrich. All solutions were prepared using Milli-Q water.

QCM Measurements. The QCM system consisted of a phase lock oscillator (PLO-10i, Maxtek, East Syracuse, New York) and a frequency counter (53131A, Agilent Technologies, Santa Clara, CA). Quartz crystals (5 MHz) with Au deposited on both sides were purchased from Inficon (East Syracuse, New York). The crystals were cleaned in piranha solution for 30 s, then rinsed with Milli-Q water, and finally dried under nitrogen flow before each use. A flow cell, FC-550 (Inficon), was installed on the crystal to create a flow chamber of approximately 0.1 mL. Solutions were pumped through the flow cell by a syringe pump (New Era Pump Systems Inc., Farmingdale, NY). Typically, a stable baseline was achieved 1 h after flow injection on a clean crystal at a flow rate of 50 μL/min.

Electrochemical Measurements. All the electrochemical measurements were performed with a μAUTOLAB potentiostat (Type III, FRA2, Metrohm Autolab, Netherlands). A gold wire (diameter 1 mm) sealed in epoxy and a platinum mesh were used as the working and counter electrode, respectively. The potentials were measured vs Ag/AgCl reference electrode. Both cyclic voltammetry and EIS measurements were conducted in a solution of 1 mM ferro/ferricyanide in 0.1 M sodium perchlorate, except for the redox-free impedance measurement.

The working electrodes were polished with 1 μm alumina slurry, sonicated, and rinsed thoroughly with water before each use. The cleaned electrodes were further tested in 0.1 M H_2SO_4 by scanning the potential between −0.5 and 1.4 V until reproducible scan results were obtained. Typically, the gold electrodes were immersed in 0.1 mM peptide solution for 1 h and then rinsed with water. The Au−pep electrodes were subsequently immersed in 1 mM cysteine solution for 2 h to block any remaining bare Au surface. After that, the Au−pep−cys electrodes were taken out of the cysteine solution and transferred to the ferro/ferricyanide solution for the cyclic voltammetry and EIS measurements. After the electrochemical measurement, the Au−pep−cys electrodes were incubated in TnI solution for 1 h. Finally, the Au−pep−cys−TnI electrodes were removed, rinsed, and transferred back to the ferro/ferricyanide solution for the final electrochemical measurements.

CV experiments were performed at a scan rate of 100 mV/s. Impedance spectra were recorded over a frequency range of 0.1−10^5 Hz. Impedance at 115 Hz was measured in the time-course measurements. A single sinusoidal AC voltage of 10 mV was superimposed on the open-circuit potential (typically 0.22 V vs Ag/AgCl).

RESULTS AND DISCUSSION

Sensor Preparation. A short peptide (TnPep) with amino acid sequence of FYSHSFHENWPS has previously been identified and characterized.[23] The peptide was found to specifically bind to TnI when five copies of these peptides were displayed on polyvalent phage particles. In order to use this peptide in the development of a TnI biosensor, the peptide has been modified with a C-terminal cysteine for immobilization on gold.

The preparation steps of the sensors are shown in Figure 1. The formation of the sensing layer includes the immobilization of the peptide (step 1, Figure 1) and blocking of empty sites with cysteine (step 2, Figure 1). Both processes were monitored by QCM and electrochemical (CV and EIS) measurements.

The total frequency change, Δf, of the QCM crystal immersed in a liquid containing the binding analyte is

$$\Delta f = \Delta f_m + \Delta f_L \quad (1)$$

where Δf_m and Δf_L are the frequency changes due to mass loading and liquid viscosity/density change. The mass change at the QCM crystal surface (Δm) can be calculated according to the Sauerbrey equation:[60]

$$\Delta f_m = -C_f \times \Delta m \quad (2)$$

where $C_f = 0.0566$ Hz/(ng/cm^2) for a 5 MHz AT-cut crystal at 20 °C.

When the QCM comes in contact with a liquid, there is a decrease in frequency that is dependent on the viscosity η_L and density of the solution ρ_L based on Kanazawa's solution.[61] Liquid loading also causes an increase in series resonance resistance, R, of the crystal. A Butterworth−Van Dyke equiva-

(59) Hessel, M. H. M.; Michielsen, E.; Atsma, D. E.; Schalij, M. J.; van der Valk, E. J. M.; Bax, W. H.; Hermens, W. T.; van Dieijen-Visser, M. P.; van der Laarse, A. *Exp. Mol. Pathol.* **2008**, *85*, 90–95.

(60) Sauerbrey, G. *Z. Phys.* **1959**, *155*, 206–222.

(61) Kanazawa, K. K.; Gordon, J. G. *Anal. Chim. Acta* **1985**, *175*, 99–105.

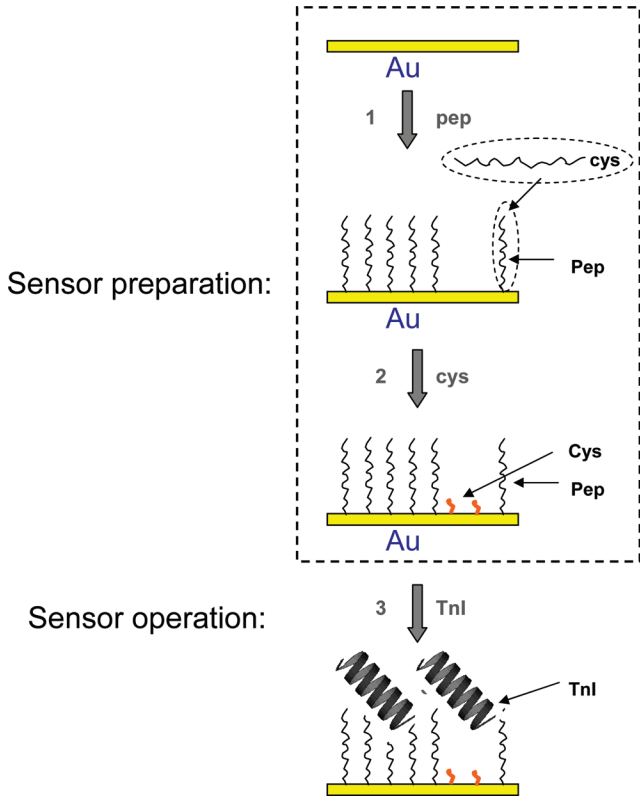

Figure 1. Schematic diagram illustrating the surface preparation and binding steps used for the biosensor: (1) immobilization of peptide, (2) blocking with cysteine, and (3) binding and detection of target (TnI). All steps were studied with QCM and electrochemistry (EIS and CV).

lent circuit model[62] has been applied to derive a linear relationship between the change in series resonance resistance, ΔR, and $(\eta_L\rho_L)^{1/2}$.[63,64] Since both Δf_L and ΔR are proportional to $(\eta_L\rho_L)^{1/2}$, the QCM manufacturer (Maxtek, East Syracuse, New York) gives an experimentally derived relationship between Δf_L and ΔR as shown in eq 3

$$\Delta R = -\kappa \Delta f_L \tag{3}$$

where $\kappa = 0.5\ \Omega$/Hz.

Since ΔR is caused only by the change of viscosity, it can be used as an independent indicator of the near-surface viscosity change induced by the structural change of the surface layer. Thus, Δf_L can be easily calculated from eq 3 and subtracted from the total observed change of frequency to give a more refined estimate of mass loading according to eq 1.

A cysteine anchor was attached at the C-terminal end of the TnI-binding peptide to immobilize the peptide on Au (step 1, Figure 1). The immobilization was observed by a large (12.7 Hz) frequency drop of the QCM when the peptide buffer solution arrived at the cell (Figure 2A, $t = 0$). Despite the large frequency change, Δf, only a small corresponding resistance change ($\Delta R \approx 0.65\Omega$, corresponding to $\Delta f_L = 1.3$ Hz based on eq 3) was measured (Figure 2B). As discussed in the previous section, the frequency change resulting from rigid-mass loading can be separated from the total observed frequency change. The $\Delta f_L = 1.3$ Hz due to the local viscosity change was subtracted from the total frequency change of 12.7 Hz, resulting in $\Delta f_m = 11.4$ Hz. According to eq 2, the mass loading of immobilized peptide per area is, therefore, about 201 ng/cm^2, which, with a molecular weight of 1640.8 g/mol, gives a peptide packing density of 1.2×10^{-10} mol/cm^2 or 7.4×10^{13} molecule/cm^2. The surface density of peptide monolayers prepared by attaching the peptide onto a self-assembled monolayer on Au via thiol−disulfide exchange reactions has been reported to be 1.5×10^{13} molecules/cm^2.[65] Inamori et al. report a surface density of 1.8×10^{12} to 1.8×10^{13} molecules/cm^2, depending on the attachment methods for the immobilized peptide on amino-modified Au.[66] Both studies involved use of a linker between the gold surface and the peptide instead of the direct binding of the peptide onto gold, as in our case. The slightly denser peptide packing obtained in our study may be due to the direct bonding of peptide on the surface via the cysteine anchor or the smaller size of the peptide we used. The average cross-section of each peptide was ~1.4 nm^2 based on the surface density, which indicates a dense packing mode of the immobilized peptides. The subsequent rinse of buffer caused a small frequency increase and resistance decrease ($\Delta f \approx 3$ Hz, $\Delta R \approx 1.2\Omega$, or $\Delta f_L = 2.4$ Hz; the vertical drop observed at the injection of buffer was caused by the sudden pressure change due to valve switching). Since Δf is comparable to Δf_L, these changes were probably due to the viscosity change upon switching to buffer.

After the immobilization of peptide, a solution of cysteine (1 mM) was introduced to block the empty sites of the gold surface. As shown in Figure 2A, a very small frequency drop followed by a frequency increase of about 6.3 Hz was observed. In contrast to the peptide immobilization step, a large change in resistance was observed in the cysteine blocking process. The initial small drop of frequency suggests the backfilling of cysteine onto empty sites, with a concomitant increase in surface mass during this short time period. The following frequency increase and resistance decrease over the next 2 h can be analyzed using the same strategy described in the peptide case above. Since $\Delta f \approx 6.5$ Hz and $\Delta R \approx 3.3\Omega$ (corresponding to $\Delta f_L = 6.6$ Hz) during this step, it seems that almost all the frequency change is due to the changes in the near-surface physical properties of the liquid layer; i.e., Δf is approximately equal to Δf_L, as opposed to changes in mass loading. Mantzila et al. attributes the change in impedance that occurs after blocking the free sites on the peptide−Au layer to a change in conformation of the immobilized peptide and to desorption.[45] Our QCM data suggest the change in conformation is the main reason for the observed frequency change. We hypothesize that the cysteine attachment causes the bound peptide to orient perpendicular to the surface.

EIS measurements at a fixed frequency of $f = 115$ Hz were used as an additional technique to monitor the surface preparation. First, the bare Au electrode was incubated in the solution of TnPep, and the impedance at 115 Hz was recorded over time. Figure 2 shows that both the real ($Z' \sim R$, Figure 2C) and

(62) Geelhood, S. J.; Frank, C. W.; Kanazawa, K. *J. Electrochem. Soc.* **2002**, *149*, H33–H38.
(63) Muramatsu, H.; Tamiya, E.; Karube, I. *Anal. Chem.* **1988**, *60*, 2142–2146.
(64) Martin, S. J.; Spates, J. J.; Wessendorf, K. O.; Schneider, T. W.; Huber, R. J. *Anal. Chem.* **1997**, *69*, 2050–2054.
(65) Wegner, G. J.; Lee, H. J.; Corn, R. M. *Anal. Chem.* **2002**, *74*, 5161–5168.
(66) Inamori, K.; Kyo, M.; Matsukawa, K.; Inoue, Y.; Sonoda, T.; Tatematsu, K.; Tanizawa, K.; Mori, T.; Katayama, Y. *Anal. Chem.* **2008**, *80*, 643–650.

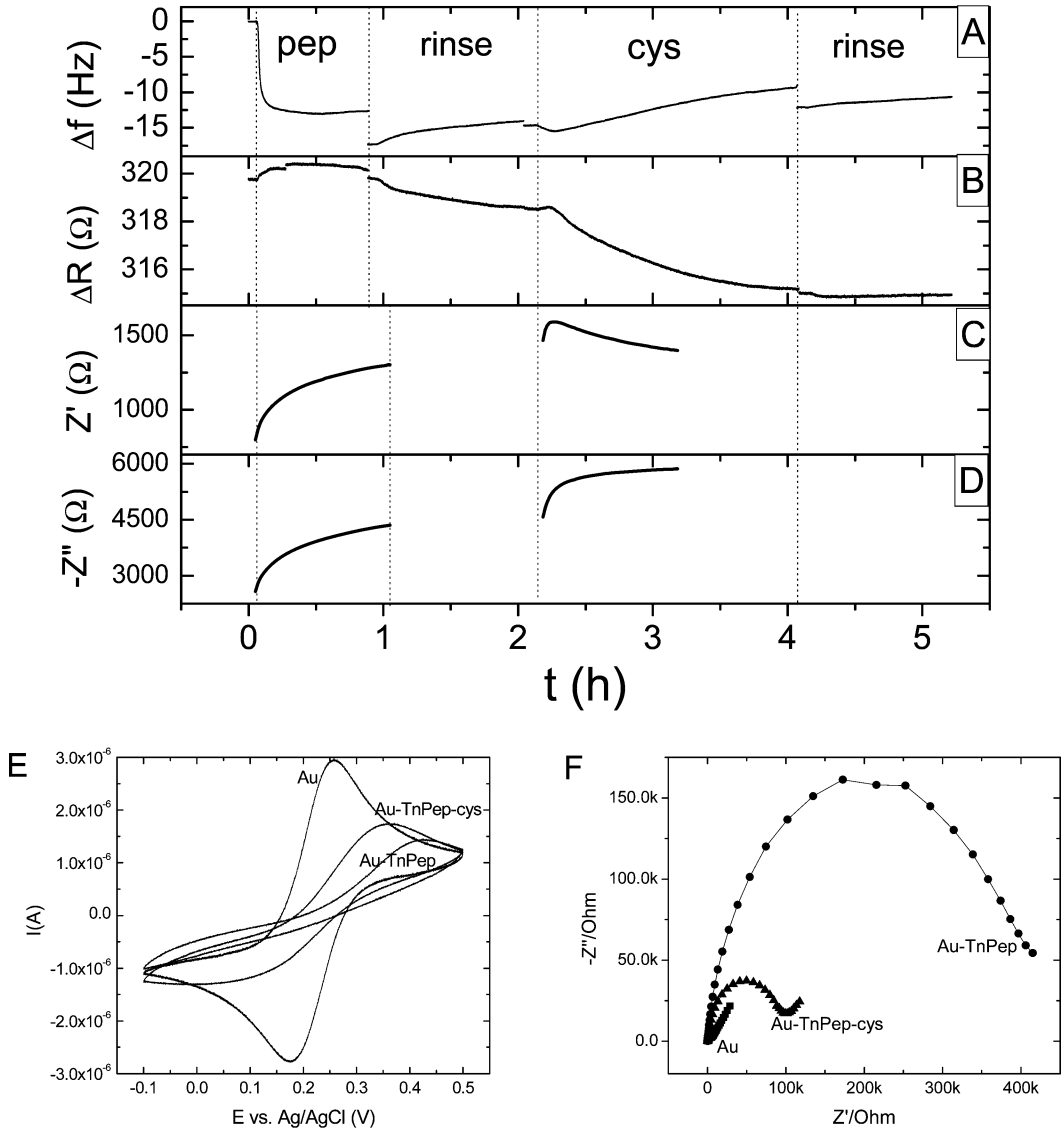

Figure 2. Change in frequency (panel A), crystal resistance (panel B), and impedance at $f = 115$ Hz (real component Z', panel C; imaginary component Z'', panel D) during the immobilization of TnPep (0.1 mM) and subsequent blocking with cysteine (1 mM) on Au. CV (panel E) and EIS (panel F) in 1 mM solution of $Fe(CN)_6^{4-/3-}$ in 0.1 M $NaClO_4$ are also shown.

imaginary ($Z'' \sim 1/\omega C$, Figure 2D) components of the impedance, Z, increased with time during the formation of the TnPep self-assembled monolayer (SAM). Results indicate that the immobilization occurs rapidly within the first few minutes and approaches a plateau within 1 h. The TnPep−Au was then removed, rinsed, and transferred to the cysteine solution for the blocking procedure. Figure 2 shows that Z'' ($\sim 1/\omega C$, Figure 2D) increases with time, as in the TnPep case, while Z' (Figure 2C) increased over the first 10 min and decreased afterward. These two steps in the change in Z' may be explained by the initial backfilling of cysteine on the surface, followed by a reorganization of the immobilized TnPep. Similar phenomenon was observed in the QCM experiments.

Usually, a faradaic impedance measurement involving a redox couple offers higher sensitivity than a probe-free nonfaradaic measurement.[45,46,53] A $Fe(CN)_6^{4-/3-}$ redox couple was used as the probe. The prepared TnPep−Au electrode was rinsed and transferred to a $Fe(CN)_6^{4-/3-}$ solution for electrochemical measurements. After cysteine blocking, electrochemical measurements were repeated. The charge transfer between $Fe(CN)_6^{4-/3-}$ and the electrode occurs either by tunneling of electrons through the surface SAM (TnPep or cysteine) or through the defects (unblocked sites) on the surface.[42] Therefore, the impact of surface passivation on charge transfer serves to decrease the peak current in CV or increase the charge transfer resistance (R_{CT}) in EIS. Figure 2 shows the cyclic voltammograms (panel E) and Nyquist plots of the EIS (panel F) of bare Au, Au−TnPep, and Au−TnPep−cys electrodes in $Fe(CN)_6^{4-/3-}$ solutions. The largest peak current and smallest R_{CT} was observed for the bare gold electrode. After the modification by TnPep, a dramatic decrease in current and increase in R_{CT} were seen. These results also suggest the formation of a dense monolayer of immobilized TnPep on Au. Further blocking with cysteine actually lowered the extent of surface passivation, resulting in a peak current increase and impedance decrease compared to the unblocked surface. If the addition of cysteine blocks the bare sites without changing the conformation of the previously immobilized TnPep, a higher

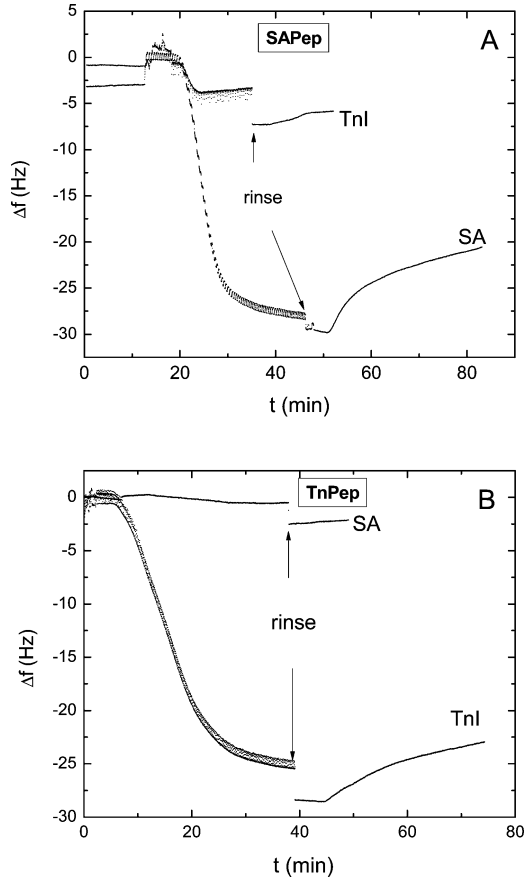

Figure 3. Shift in frequency in response to injection of TnI and SA on SAPep−cys modified Au (panel A) and TnPep−cys modified Au (panel B). The concentrations of the TnI and SA solutions were 10 μg/mL in buffer.

extent of surface passivation, resulting in a lower peak current and higher impedance, would be expected. However, our experimental results showed the opposite effect for both the current and impedance. This may again be explained by reorganization of the immobilized TnPep monolayer upon backfilling with cysteine, as suggested also in the QCM and redox-free impedance experiments.

TnI Sensor Operation. QCM, CV, and EIS measurements validate the formation of the sensing layer. The same techniques were used to demonstrate an affinity of the bound TnPep for TnI and to study the selectivity of the sensor to TnI.

As an indication of the specificity of the binding between TnPep and TnI, a second protein, streptavidin (SA), and a corresponding peptide that specifically binds to SA (SAPep)[67,68] were used as a control protein and peptide. Both TnI and SA show affinity to bare gold (data not shown), presumably due to electrostatic attractions. The SAM of cysteine on the gold surface significantly reduced the nonspecific binding (data not shown). The QCM results of TnI and SA binding to SAPep (Figure 3A) and to TnPep (Figure 3B) are shown in Figure 3. TnPep (Figure 3B) shows a large frequency change upon the introduction of TnI but almost no frequency change upon the introduction of SA. As expected, the

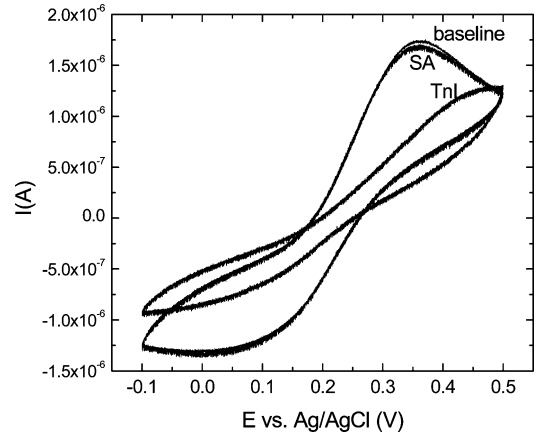

Figure 4. CVs of TnPep−cys modified Au before (baseline) and after SA and TnI binding. After incubation in 10 μg/mL SA or TnI, electrodes were transferred to a 1 mM solution of $Fe(CN)_6^{4-/3-}$ in 0.1 M $NaClO_4$ for the measurements. The scan rate was 100 mV/s.

SAPep (Figure 3A) shows the opposite behavior. When either TnI or SA solution is introduced, the SAPep demonstrated selectivity for SA, although the frequency shift indicated some affinity for TnI as well. The rinse steps demonstrated a decrease of mass on the surface, but it is not clear if this is due to some desorption of the proteins from the peptides or from the removal of nonspecifically bound proteins from the surface. These results show that binding is strong between the matched protein−peptide pairs, and considering only these combinations, the TnPep and TnI pairing is more selective than SAPep with SA. This proves that affinity properties are retained and that TnPep selected by phage display technology remains effective when immobilized on Au. The success of the transition from phage particles to the Au surface makes it possible to build a TnI biomarker sensor using this simple, synthesizable peptide film within a microfluidic chip.

To study the binding of TnPep to TnI and to allow for simple, inexpensive, portable systems, electrochemical techniques were applied in addition to QCM. SA and SAPep were again used as a control system. Figure 4 shows the CV of Au−TnPep−cys before (baseline) and after SA and TnI exposure. As shown in Figure 4, insignificant differences in current were observed before and after the electrode was exposed to SA, indicating no binding occurred between SA and TnPep. The binding of TnI with TnPep was confirmed by the large current decrease after TnI binding. The binding of bulky TnI on the sensor hinders the electron transfer, resulting in a much smaller current. The negative control of the SA test suggested that the binding between TnPep and TnI is specific.

The prepared CV samples were then rinsed and transferred to a 1 mM solution of $Fe(CN)_6^{4-/3-}$ in 0.1 M $NaClO_4$ for EIS measurements. Figure 5 shows Nyquist plots of these samples. To allow for facile data analysis, the electrochemical cell can be represented by an equivalent circuit composed of R_{CT}, a Warburg impedance Z_w, a capacitance which is represented by a constant phase element Q and resistance of solution R_{sol}, as shown in the upper right insert of Figure 5.[44,69] R_{CT} was obtained by fitting the curves in Figure 5 with EIS software using the equivalent circuit model, and the resulting R_{CT} is shown in the

(67) Korndorfer, I. P.; Skerra, A. *Protein Sci.* **2002**, *11*, 883–893.
(68) Schmidt, T. G. M.; Koepke, J.; Frank, R.; Skerra, A. *J. Mol. Biol.* **1996**, *255*, 753–766.
(69) Bard, A. J.; Faulkner, L. R. *Electrochemical Methods: Fundamentals and Applications*, John Wiley, New York, 1982.

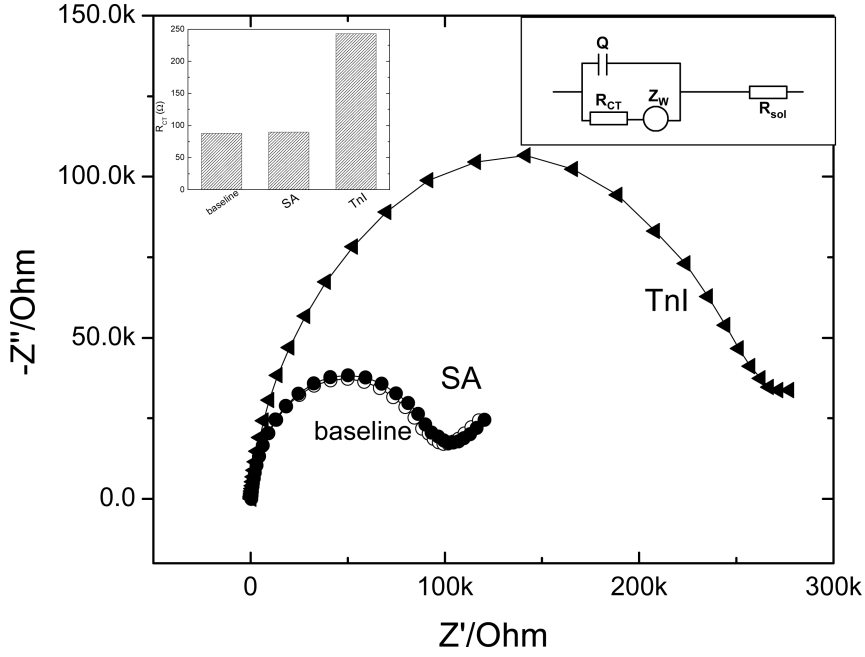

Figure 5. Nyquist plots of impedance spectra of Au−TnPep−cys before (baseline) and after SA or TnI binding. After incubation in 10 μg/mL SA or TnI, electrodes were transferred to 1 mM solution of $Fe(CN)_6^{4-/3-}$ in 0.1 M $NaClO_4$ for the measurements. Also shown are an equivalent circuit (upper right corner) and R_{CT} (upper left corner) obtained by fitting the impedance spectra with the equivalent circuit.

top left inset. Almost no difference in R_{CT} was observed for SA exposure to TnPep−modified Au, indicating no binding occurred between SA and TnPep. The binding of TnI with TnPep was suggested by the large R_{CT} increase, in agreement with the current decrease in Figure 4.

The quantitative detection of TnI at different concentrations was also performed on QCM and EIS, respectively, and the two methods are compared. The QCM frequency change as a function of TnI concentration is summarized in Figure 6A. The apparent amount of bound TnI, N_{TnI}, estimated from eqs 1−3, is also shown on the right ordinate. A higher sensitivity was observed at concentrations below 1 μg/mL. The sensitivity in the lower concentration region (<1 μg/mL) is calculated to be ~18 Hz/(μg/mL) based on the slope of the fitted line in this region. The corresponding surface density of TnI bound on TnPep is between 4×10^{-12} and 2×10^{-11} mol/cm^2 in the studied concentration range. Since the surface density of TnPep has been estimated as 1.2×10^{-10} mol/cm^2 in Sensor Preparation, the molar ratio of TnPep to TnI is between 30:1 and 6:1 in the TnI concentration range of 0.25−6 μg/mL.

The quantitative relationship between TnI concentration and R_{CT} measured in EIS was also characterized. There are two methods to perform a response test: a sequential dose injection on one electrode or independent tests on different electrodes in parallel. The latter method is closer to a normal testing protocol and is more stringent because it requires identical electrode morphologies and modifications. Usually, this is difficult to achieve in practice and poor reproducibility has been reported in many cases.[47,54] We performed both methods in buffer solutions in our study, and the results are shown in Figure 6B. To best simulate a potential biosensor environment, additional tests were made using solutions of TnI in Minimum Essential Media (MEM) which is a widely used synthetic cell culture media. A normalized change in R_{CT} was chosen to characterize the

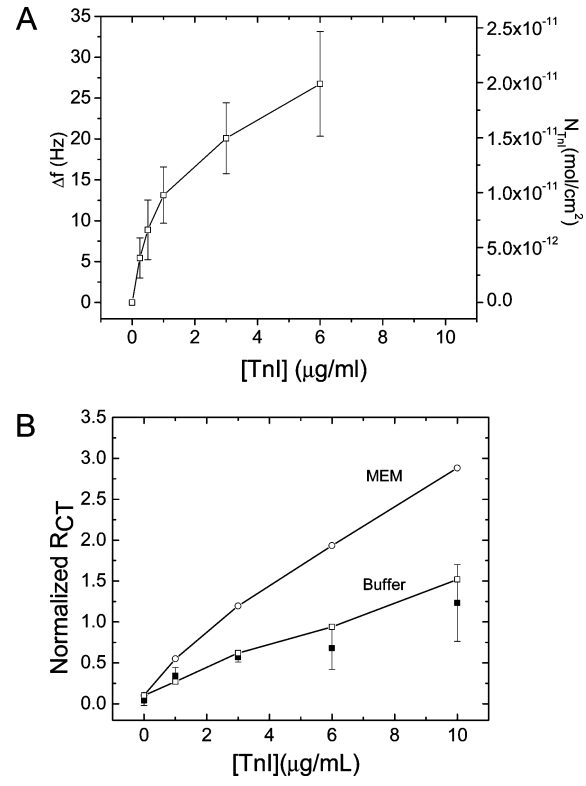

Figure 6. Response curves of TnI binding as determined by QCM (panel A) and EIS (panel B). Filled squares are results obtained from electrodes tested in parallel. Open symbols are results obtained from one electrode under successive tests in TnI solutions in buffer (open square) and in Minimum Essential Media (MEM) (open circle) from low to high concentration. Error bars represent standard deviations obtained from triplicate measurements.

signal response to minimize the individual differences between samples. Sensors tested in both media show small responses (<4% for buffer and <10% for MEM) to blank samples containing

no TnI. Larger error bars were observed at higher concentration ranges. The sensitivity (defined as the slope of the calibration curve) and limit of detection (LOD, defined as the average blank value plus 3 times the value of the standard deviation of the blank value, converted to TnI concentrations)[70] for QCM measurements were determined to be

$$\text{Sensitivity (at} < 1\,\mu\text{g/mL)} = 18 \pm 1\,\text{Hz}/(\mu\text{g/mL})$$
$$\text{LOD} = 0.11\,\mu\text{g/mL}$$

and for EIS:

$$\text{Sensitivity (at} < 3\,\mu\text{g/mL)} = 0.30 \pm 0.030\,\text{normalized impedance}/(\mu\text{g/mL})$$
$$\text{LOD} = 0.34\,\mu\text{g/mL}$$

These LOD values are significantly higher than those reported for commercial TnI assays (<0.1 ng/mL) which use antibody-based platforms.[9] Larger signals were obtained for samples in MEM than those in buffer throughout the tested concentration range, indicating an increased sensitivity in this milieu.

Compared to the response curves in QCM, the EIS curve was more linear across the 0−10 μg/mL concentration range. The response curve of any affinity biosensor arises from two separate events: the affinity step and the readout step.[54] In QCM, the signal (frequency change, Δf) is proportional to the mass loading of bound TnI. During an impedance measurement, the signal (R_{CT}) is directly related to surface passivation or the hindrance of interfacial electron transfer. At high concentration, impedance may still increase significantly even though the amount of bound TnI only increases by a small amount if the binding of additional TnI results in a large change in the interfacial electron transfer impedance.

Another complicating factor is whether the binding is controlled kinetically or reaches equilibrium during the experiment.[54] In QCM, the Δf−time curve can be monitored throughout the experiments to determine whether the binding reaches a steady state. In contrast, impedance measurements are performed at a single time point. In this case, the samples were left in TnI solutions at different concentrations for 1 h. At low concentrations of TnI, the binding may not have reached the equilibrium in 1 h.

Kinetics of TnI Binding on QCM. The QCM data can be used to directly study the kinetics of TnI binding by TnPep. The equilibrium dissociation constant, K_d, can be obtained via two independent methods[41,71,72] either from estimation of k_{on}/k_{off} or from equilibrium calculations. A plot of $d(\Delta f)/dt$ vs Δf gives a line with slope of $-(k_{on}C + k_{off})$ or τ^{-1} where τ is the relaxation time of binding. If τ^{-1} is plotted against C for various concentrations of TnI, the resulting slope is equal to k_{on} and the intercept is equal to k_{off}. The dissociation constant K_d can then be calculated since $K_d = k_{off}/k_{on}$. Alternatively, when binding reaches equilibrium (the plateau in the Δf vs t curve), the plot of frequency change, Δf_{eq}, vs $\Delta f_{eq}/C$ gives a slope of K_d.

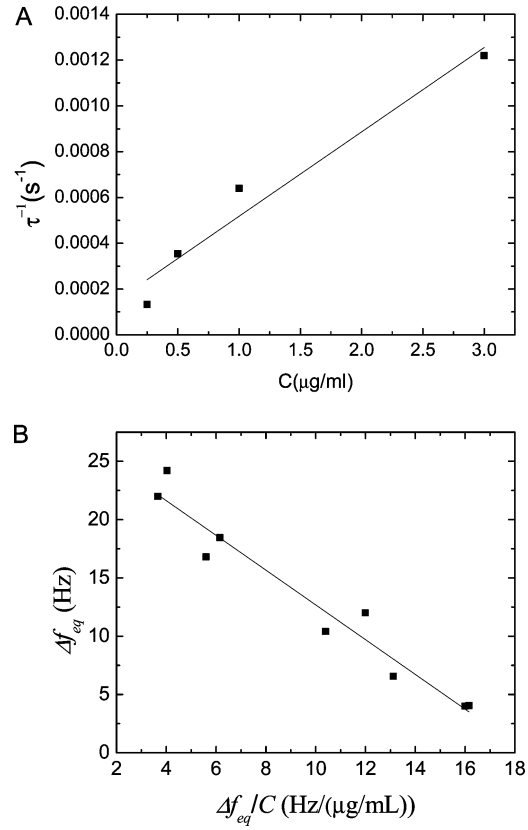

Figure 7. Kinetic constants of TnI binding to TnPep as determined from kinetic and equilibrium analysis of QCM measurements. (Panel A) τ^{-1} vs TnI concentration C, $k_{on} = (8.9 \pm 1.2) \times 10^3\ M^{-1}s^{-1}$, $k_{off} = (1.5 \pm 0.9) \times 10^{-4}\ s^{-1}$, and $K_d = 17 \pm 8$ nM. (Panel B) at equilibrium, Δf_{eq} vs $\Delta f_{eq}/C$ and $K_d = 66 \pm 4$ nM. The errors of all constants were obtained from linear regression.

Both methods were used in this work to calculate K_d. The plots of k vs C (panel A) and Δf_{eq} vs $\Delta f_{eq}/C$ (panel B) are shown in Figure 7. The on and off rate constants and the equilibrium dissociation constant obtained from the first method are $k_{on} = (3.7 \pm 0.5) \times 10^{-4}\ (\mu g/mL)^{-1}s^{-1}$ or $(8.9 \pm 1.2) \times 10^3\ M^{-1}s^{-1}$, $k_{off} = (1.5 \pm 0.9)\ 24 > 10^{-4}\ s^{-1}$, and $K_d = 0.4 \pm 0.2\ \mu g/mL$ or 17 ± 8 nM. The equilibrium dissociation constant obtained from the equilibrium state is $K_d = 1.5 \pm 0.1\ \mu g/mL$ or 66 ± 4 nM. The equilibrium dissociation constant of TnPep on phage is $K_d = 2.5 \pm 0.1$ nM, which indicates a better binding of TnI by the peptides on the phage particles, as compared to the same peptides immobilized on gold. When peptides are immobilized on M13 phage particles, five copies of the peptide are displayed in close proximity on one end of the phage particles. The selection process may favor multiple interactions between the peptides and the TnI target that could be facilitated by the structure of the phage particles. When the peptides are transferred to the gold surface, it is possible that the conformational arrangements of the peptides are altered, leading to reduced avidity and/or affinity for the target protein.

When $C_{TnI} \gg K_d$, θ (surface coverage of TnI) $\ll 1$ and the response saturates. For $C_{TnI} \ll K_d$, θ is proportional to C_{TnI}. In the QCM, since the readout Δf is proportional to θ, one would expect the QCM sensor output to be proportional to the target concentration C_{TnI} in the low-concentration regime. This agrees with the response curve using QCM in Figure 6A.

(70) Gonzalez, A. G.; Herrador, M. A. *TrAC, Trends Anal. Chem.* **2007**, *26*, 227–238.
(71) Felder, S.; Zhou, M.; Hu, P.; Urena, J.; Ullrich, A.; Chaudhuri, M.; White, M.; Shoelson, S. E.; Schlessinger, J. *Mol. Cell. Biol.* **1993**, *13*, 1449–1455.
(72) Payne, G.; Shoelson, S. E.; Gish, G. D.; Pawson, T.; Walsh, C. T. *Proc. Natl. Acad. Sci. U.S.A.* **1993**, *90*, 4902–4906.

Comparison of QCM, CV, and EIS. QCM, CV, and EIS were used in our study as the measurement techniques for developing a TnI biosensor. All three techniques show that the peptide is specific for TnI as compared to the SA control protein. CV measurements failed to give a quantitative response due to the extremely small current passed on the highly passivated surface upon binding of TnI. Both QCM and EIS demonstrated quantitative responses to TnI in the concentration range of 0−10 μg/mL. The LOD of QCM (0.11 μg/mL) is lower than that of EIS (0.34 μg/mL). However, the lower LOD is mainly due to the lower background noise level that can be achieved using QCM. In QCM, which is operated using a flow cell, the blank buffer solution can be introduced by switching valves. In contrast, the EIS electrodes were prepared in blank buffer solution, rinsed, and transferred to $Fe(CN)_6^{4-/3-}$ solutions for measurements. EIS, however, demonstrates a larger linear dynamic range than QCM. Considering the development of a biosensor that can be used in field, EIS is easier to integrate into a device than a QCM probe because the QCM requires highly stable temperature and pressure controls and may involve more complex microfabrication routes. EIS measurements were faster and simpler than the QCM measurements, but a significant limitation is the need for the addition of the $Fe(CN)_6^{4-/3-}$ solution prior to measurement. Overall, EIS is a more appealing choice than QCM for a deployable biosensor. Nevertheless, QCM is a valuable rapid diagnostic tool for laboratory use for target recognition since it simply responds to changes in surface mass loading (target binding) and is a real-time monitoring technique.

CONCLUSIONS

In this work, a small synthetic peptide identified from a polyvalent phage displayed library was immobilized on a gold surface via an attached cysteine moiety. The affinity of the immobilized peptide for TnI was studied by QCM, CV, and EIS. All three techniques indicate that the immobilized peptide binds the TnI protein target, and therefore, the TnI peptide is a valuable recognition sequence for this important biomarker of heart trauma.

To deploy this peptide in a biosensor device, several alternative methods were developed and used to detect TnI at concentrations important to cell culture conditions. Among these methods, QCM and EIS show promise as a quantitative portable detection method but not CV. The response curves to TnI at concentrations between 0 and 10 μg/mL obtained in QCM and EIS were compared. QCM showed a response curve reaching saturation at high concentrations while EIS showed a more linear response over the tested concentration range with an LOD of 0.34 μg/mL. The kinetics of binding on QCM was studied by two independent analyses, and the dissociation constants (K_D = 66 nM and K_D = 17 nM) were found to be higher than that measured when the peptides remained attached polyvalently on phage particles (K_D = 2.5 nM). In the MEM tissue culture media, a higher sensitivity of the EIS measurements was obtained as compared to measurements made in buffer. The ability to respond to TnI in complex MEM makes the combination of TnPep and EIS extremely attractive as the recognition scheme for troponin release from cardiac cell culture upon toxin exposure in a microfluidic format.

To the best of our knowledge, this is the first example of the use of TnI binding peptides obtained from polyvalent phage display for TnI sensor development. These results may enable new sensing probes for detecting cardiac biomarkers as well as providing a general example for application of affinity peptides identified from phage display libraries to sensor development.

ACKNOWLEDGMENT

This research was supported by U.S. Army Corps of Engineers Applied Research program with funding from the U.S. Army Engineering Research and Development Center, Construction Engineering Research Laboratory (ERDC-CERL).

Received for review June 24, 2010. Accepted August 28, 2010.

AC101657H